Characterization of the natural barriers of intergranular tunnel junctions: Cr 2 O 3 surface layers on CrO 2 nanoparticles

Jianbiao Dai, Jinke Tang, Huiping Xu, Leonard Spinu, Wendong Wang, Kaiying Wang, Amar Kumbhar, Min Li, and Ulrike Diebold

Citation: Applied Physics Letters **77**, 2840 (2000); doi: 10.1063/1.1320845
View online: http://dx.doi.org/10.1063/1.1320845
View Table of Contents: http://scitation.aip.org/content/aip/journal/apl/77/18?ver=pdfcov
Published by the AIP Publishing

Characterization of the natural barriers of intergranular tunnel junctions: Cr_2O_3 surface layers on CrO_2 nanoparticles

Jianbiao Dai[a] and Jinke Tang[b]
Department of Physics, University of New Orleans, New Orleans, Louisiana 70148

Huiping Xu, Leonard Spinu, Wendong Wang, Kaiying Wang, and Amar Kumbhar
Advanced Materials Research Institute, University of New Orleans, New Orleans, Louisiana 70148

Min Li and Ulrike Diebold
Physics Department, Tulane University, New Orleans, Louisiana 70118

(Received 25 May 2000; accepted for publication 6 September 2000)

Cold-pressed powder compacts of CrO_2 show large negative magnetoresistance (MR) due to intergranular tunneling. Powder compacts made from needle-shaped nanoparticles exhibit MR of about 28% at 5 K. Temperature dependence of the resistivity indicates that the Coulomb blockade intergranular tunneling is responsible for the conductance at low temperature. In this letter we report direct observation and characterization of the microstructure of the intergranular tunnel barriers, using transmission electron microscopy, x-ray diffraction (XRD), and x-ray photoelectron spectroscopy (XPS). A very thin native oxide layer with a thickness of 1–3 nm on the surface of CrO_2 powders has been observed. The composition and crystal structure of this surface layer has been determined to be Cr_2O_3 by XPS and XRD. The dense and uniform Cr_2O_3 surface layers play an ideal role of tunnel barriers in the CrO_2 powder compacts. © *2000 American Institute of Physics.* [S0003-6951(00)00344-2]

The magnetotransport properties of chromium dioxide (CrO_2) have attracted much attention recently because it was predicted to be a half-metallic ferromagnet by band structure calculation.[1] Several experiments support the half-metallicity.[2–4] The high degree of spin polarization of the electrons at the Fermi level suggests that CrO_2 could be an ideal material for the magnetic tunneling devices. Extremely high values of magnetoresistance (MR) may be reached, which have been reported in several experiments on CrO_2 polycrystalline films and powder compacts.[5–8] Manoharan *et al.*[5] reported a 30% negative MR of cold-pressed CrO_2 powder sample at 4.2 K. Coey *et al.*[6] also reported a ~30% MR of cold-pressed CrO_2 powder compacts and a 50% MR of a dilute composite sample at 5 K.

The conduction mechanism of the above CrO_2 structures is due to the spin dependent intergranular tunneling affected by the Coulomb gap,[6] and the grain boundaries are believed to play the role of the tunnel barriers of the intergranular tunneling. The grain boundaries are suspected to be made of a native Cr_2O_3 layer on the surfaces of CrO_2,[6,7,9] since it is the most stable phase of CrO_x.[2,6,10] It is suggested in Ref. 6 that the boundary layer can be the thermodynamically stable oxide Cr_2O_3. Huang and Cheong[7] also suggest that the Cr_2O_3 at the interface act as a tunnel barrier. However, this intergranular tunnel barrier has not been carefully examined before and its nature is not precisely known. It is also possible that the grain boundary, or surface layer, is made of amorphous CrO_2,[2,11] or even compounds like CrOOH.[12] It is obviously important to learn the microstructure of the grain boundaries and surface layers, and to understand why they work extremely well as the tunnel barriers.

In this work, we have studied the microstructure of the surface layers of the CrO_2 particles using transmission electron microscopy (TEM), and x-ray diffraction (XRD) and x-ray photoelectron spectroscopy (XPS). We report direct observation by TEM of a 1–3 nm thick native oxide layer on the surface of the CrO_2 single crystal powders, which has been characterized as crystalline Cr_2O_3. This layer is believed to play the role of tunnel barrier in the intergranular tunneling effect in the CrO_2 powder compacts.

Samples used in our experiments were made from CrO_2 powders supplied by DuPont. The powders have been analyzed by XRD and TEM. They are single crystal needle-shaped particles with length of about 400 nm and an aspect ratio of about 9:1. The coercivity is about 600 Oe at room temperature and about 1000 Oe at $T=5$ K. Cold-pressed CrO_2 compacts were made under a pressure of 5×10^8 N/m^2. The electron transport properties were measured using a Quantum Design physical properties measurement system (PPMS) in magnetic fields from -5 to 5 T over the temperature range from 5 to 300 K.

The resistivity of the cold-pressed CrO_2 powder compact is about 0.1 Ω cm. Figure 1 shows the negative MR at 5 K, where the MR is defined as $(R_H-R_{H=0})/R_{H=0}$. It reaches about 28% in a field of 5 T. The inset of Fig. 1 shows the low field MR and magnetic hysteresis loop which exhibit clear correlation between the two. Figure 2 shows the resistance R as a function of temperature T, and in the inset $\ln R$ is plotted against $T^{1/2}$. The resistance R has been normalized to the value at $T=300$ K. One can see that $\ln R$ is linear to $1/T^{1/2}$ at low temperature, which is typical of intergranular tunneling. The spin dependent tunneling across the interface between

[a]Also at Dept. of Applied Physics, Jiao Tong University, Shanghai, People's Republic of China, electronic mail: jdai@uno.edu
[b]Electronic mail: jtang@uno.edu

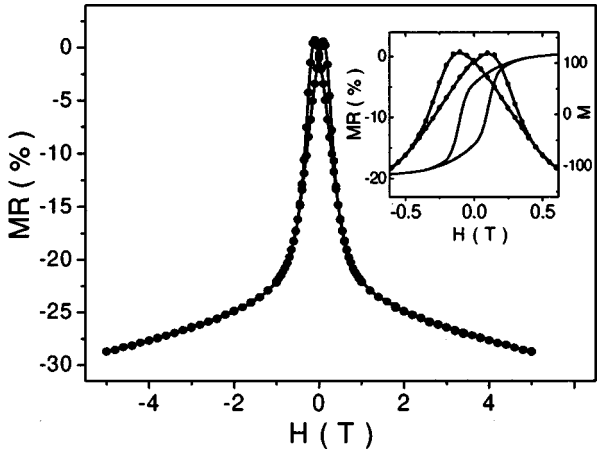

FIG. 1. MR of the cold-pressed CrO_2 powder compact at $T=5$ K. Inset shows the low field MR and hysteresis loop.

two neighboring CrO_2 particles is understood as intergranular tunneling with a Coulomb gap.[6] The resistance as a function of temperature can be expressed as[13–15]

$$R \propto \exp(\Delta/T)^{1/2}, \tag{1}$$

where Δ is proportional to the Coulomb charging energy E_c and tunnel barrier thickness s. In our CrO_2 sample, Δ determined from the slope of Fig. 2 inset is found to be about 6 K, which is in reasonable agreement with the value estimated from the particle size and barrier thickness.[13] The data in Fig. 2 fit Eq. (1) very well and imply the intergranular tunneling is the major mechanism of the conductance at low temperature.

TEM analysis has been performed to characterize the microstructure of the single crystal CrO_2 particles as shown in Figs. 3(a)–3(d). Figure 3(a) shows the CrO_2 particles of needle shape with a diameter of ~50 nm. A very thin surface layer can be seen on each particle in the TEM image with higher magnification as shown in Fig. 3(b). Figure 3(c) is a high resolution lattice image of the CrO_2 particle with [001] axis along its length, showing clearly the thin layer on the surface of the single crystal lattice image of CrO_2. By means of XPS, one can identify the composition of this surface layer to be Cr_2O_3, the details of which will be discussed later. The corresponding electron diffraction pattern of the

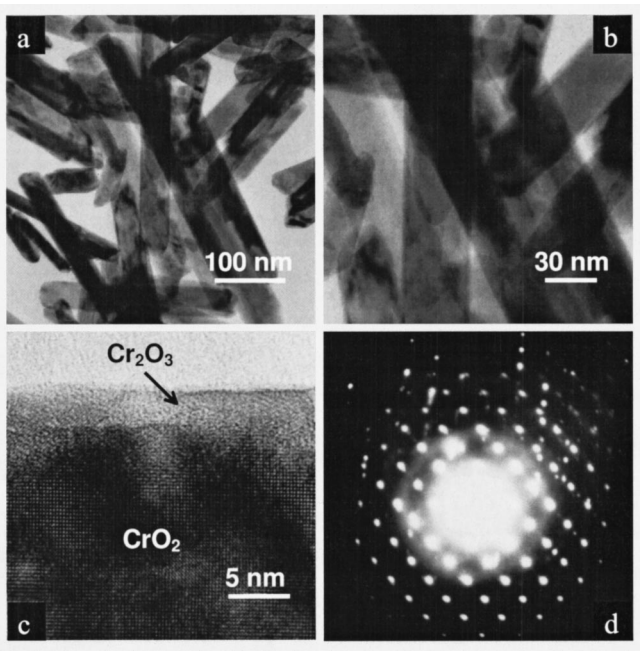

FIG. 3. (a) TEM micrographs of needle shaped CrO_2 particles; (b) enlarged micrograph; (c) high-resolution image of the particle; (d) electron diffraction pattern.

CrO_2 particle is shown in Fig. 3(d) and the ring-shaped background is from the Cr_2O_3 surface layer. The diffuse electron diffraction pattern of Cr_2O_3 is because the native oxide layer is very thin (1–3 nm) and mostly of low degree of crystallinity.

XPS measurements were performed in a separate UHV chamber with a base pressure of 10^{-10} Torr. CrO_2 powders and standard Cr_2O_3 powders were cold pressed and mounted on sample holders. The Cr_2O_3 sample is used as a standard for comparison of the Cr $2p$ peak with the CrO_2 sample. As shown in Fig. 4, the similarity of the Cr $2p$ peak shapes between CrO_2 and Cr_2O_3 suggests that the Cr^{3+} dominates in the near surface region (~10 ML) of the CrO_2 particles. One should notice that XPS is sensitive within 10–20 Å into the particle surface. Our result indicates that the 1–3 nm thick surface layer on the CrO_2 particles is not CrO_2 but a Cr^{3+} compound. The result strongly supports the expectation that

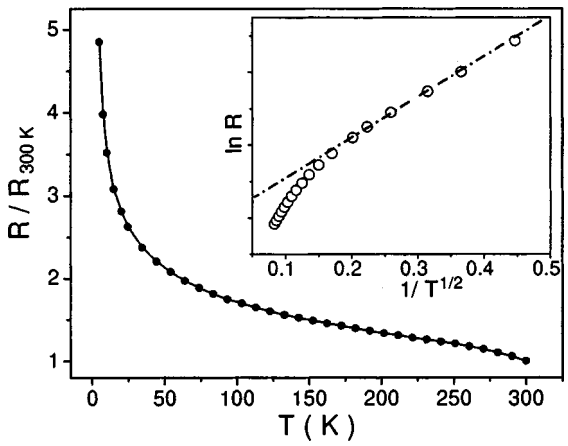

FIG. 2. Resistance R as a function of temperature. Inset shows the ln R as a function of $1/T^{1/2}$ and linear relationship exists at low temperature.

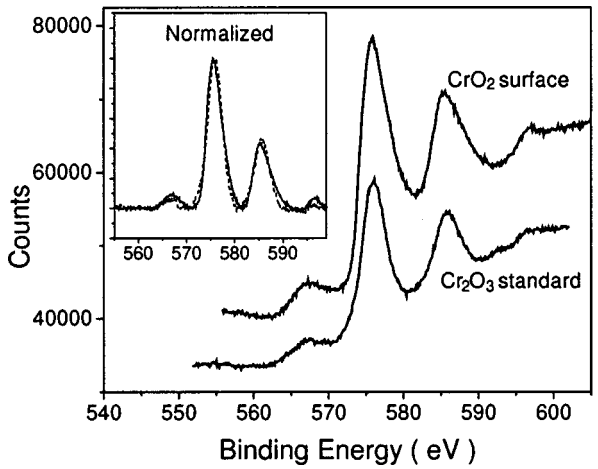

FIG. 4. XPS Cr $2p$ peaks of CrO_2 and Cr_2O_3 standard (dashed line in the inset).

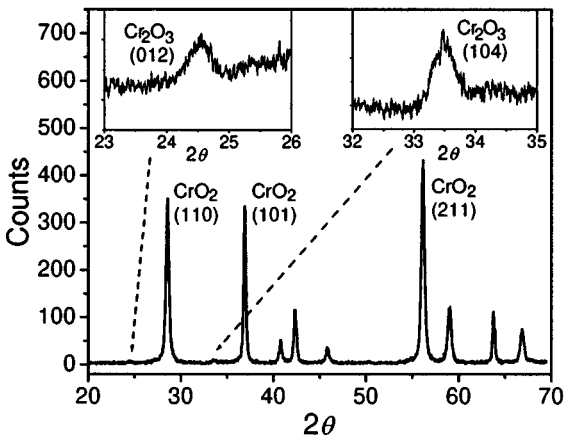

FIG. 5. X-ray diffraction pattern of the CrO_2 powders. Inset shows the detailed scan over the range $23° < 2\theta < 26°$ and $32° < 2\theta < 35°$. Peaks corresponding to the (012) and (104) reflections of Cr_2O_3 are shown.

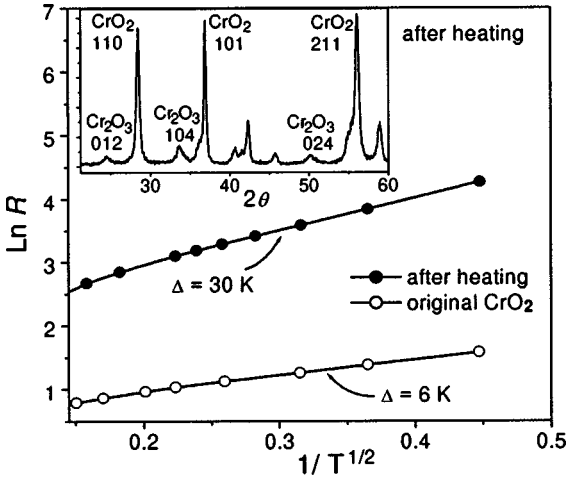

FIG. 6. $\ln R$ as a function of $1/T^{1/2}$ at low temperature for CrO_2 sample (○) and the sample after heating at 400 °C for 20 min (●). R has been normalized to the value at $T = 300$ K. Inset shows the XRD of the heated sample showing about 20%–25% Cr_2O_3.

a Cr_2O_3 native oxide layer exists on the CrO_2 surface[6,7,9] due to the fact that Cr_2O_3 is the most stable phase of chromium oxides.[10] The high quality as seen from the TEM images and good insulating properties of Cr_2O_3 make it an ideal tunneling barrier in the spin dependent intergranular tunnel junctions of CrO_2 powder compacts.

Crystalline phases of Cr_2O_3 can be observed within the surface layer in the high-resolution TEM images, which implies the structure of the Cr_2O_3 surface layer is mostly crystalline as opposed to amorphous. Considering the 1–3 nm thickness of the Cr_2O_3 layer and the CrO_2 particle size, one can roughly estimate that there is about 5% of Cr_2O_3 in our ''pure'' CrO_2 powder samples. The CrO_2 samples were analyzed by x-ray diffraction through a detailed scan, in which very small scan steps and long scan time were used. A weak but very clear signal of Cr_2O_3 has been observed confirming the existence of Cr_2O_3 crystalline phase as is shown in Fig. 5. This XRD result further suggests that the surface layer of Cr_2O_3 is mostly made of crystalline Cr_2O_3.

Another experiment has been performed to adjust the amount of Cr_2O_3 in our sample. The CrO_2 powders were annealed in air at 400 °C for 20 min. XRD shows about 20%–25% of CrO_2 has transformed into Cr_2O_3, which is estimated from the intensity of the XRD peaks as shown in the inset of Fig. 6. This value is approximately equal to the amount of Cr_2O_3 measured by weight change of the sample. TEM shows that some CrO_2 transforms to Cr_2O_3 particles of spherical shape. Cold-pressed compacts have been made using the annealed powders. Due to the annealing, change in intergranular tunneling is expected. The resistivity increases to about 2 Ω cm, and the MR ratio of the annealed sample increases to about 33% and the slope in the $\ln R$ vs $1/T^{1/2}$ is increased as shown in Fig. 6. The Δ value in Eq. (1) is increased from 6 to 30 K accordingly. The increase in Δ is expected since it is proportional to the barrier thickness.[13–15] The annealing increases the tunnel barrier thickness probably via one of two ways: by thickening the Cr_2O_3 surface layer and by precipitating more Cr_2O_3 in the interface region.

In conclusion, we have studied the microstructure of the natural barrier layer of the spin dependent intergranular tunneling in CrO_2 powder samples. Direct observation of the barrier by TEM is reported. The barrier is a thin layer of dense and uniform crystalline Cr_2O_3 on the surface of the single crystal CrO_2 powders. The composition and crystal structure of the layer is confirmed by XRD and XPS techniques. The concentration of Cr_2O_3 and the thickness of the Cr_2O_3 surface layer can be increased by heating in air. Enhancing the properties of the oxide layer, for example, changing the thickness or impurity level of this Cr_2O_3 layer, may be helpful to obtain more desirable magnetotransport properties for applications.

The authors want to thank Dr. S. Hariharan for very helpful discussions. This work was supported by DOD/DARPA Grant No. MDA972-97-1-0003 and the Louisiana Board of Regents Support Fund, Grant No. LEQSF(2000-03)-RD-B-10.

[1] K. Schwarz, J. Phys. F: Met. Phys. **16**, L211 (1986).
[2] K. P. Kamper, W. Schmitt, and G. Guntherodt, Phys. Rev. Lett. **59**, 2788 (1987).
[3] R. J. Soulen, J. M. Byers, M. S. Osofsky, B. Nadgorny, T. Ambrose, S. F. Cheng, P. R. Broussard, C. T. Tanaka, J. Nowak, J. S. Moodera, A. Barry, and J. M. D. Coey, Science **282**, 85 (1998).
[4] R. Wiesendanper, H. J. Guntherodt, G. Guntherodt, R. J. Gambino, and R. Ruf, Phys. Rev. Lett. **65**, 247 (1990).
[5] S. S. Manoharan, D. Elefant, G. Reiss, and J. B. Goodenough, Appl. Phys. Lett. **72**, 984 (1998).
[6] J. M. D. Coey, A. E. Berkowitz, L. Balcells, and F. F. Putris, Phys. Rev. Lett. **80**, 3815 (1998).
[7] H. Y. Hwang and S. W. Cheong, Science **278**, 1607 (1997).
[8] K. Suzuki and P. M. Tedrow, Appl. Phys. Lett. **74**, 428 (1999).
[9] A. Barry, J. M. D. Coey, and M. Viret, J. Phys.: Condens. Matter **12**, L173 (2000).
[10] P. S. Robbert, H. Geisler, C. A. Ventrice, J. van Ek, S. Chaturvedi, J. A. Rodriguez, M. Kuhn, and U. Diebold, J. Vac. Sci. Technol. A **16**, 990 (1998).
[11] N. Heiman and N. S. Kazama, J. Appl. Phys. **50**, 7633 (1979).
[12] M. Essig, M. W. Muller, and E. Schwab, IEEE Trans. Magn. **26**, 69 (1990).
[13] J. Inoue and S. Maekawa, Phys. Rev. B **53**, R11927 (1996).
[14] S. Mitani, S. Takahashi, K. Takanashi, K. Yakushiji, S. Maekawa, and H. Fujimori, Phys. Rev. Lett. **81**, 2799 (1998).
[15] T. Zhu and J. Wang, Phys. Rev. B **60**, 11918 (1999).